On the oxy-combustion of lignite and corn stover in a lab-scale fluidized bed reactor

Carlos Lupiáñez[a], M. Carmen Mayoral[b], Luis I. Díez[a,1], Eloy Pueyo[a], Sergio Espatolero[a], J. Manuel Andrés[b]

[a] CIRCE, University of Zaragoza, Mariano Esquillor 15, 50018 Zaragoza, Spain

[b] Instituto de Carboquímica-CSIC, Miguel Luesma 4, 50018 Zaragoza, Spain

Abstract

This paper addresses an experimental investigation concerning oxy-combustion of coal and biomass in a lab-scale fluidized bed reactor. While co-firing has been widely studied under conventional air conditions, few experiences are available to date for O_2/CO_2 atmospheres. The research is focused on SO_2 and NO_x emissions, along with the deposition rates and ashes mineralogy. The influences of the atmosphere (air vs. 30/70% O_2/CO_2), the coal-to-biomass energy input ratio (80/20%, 90/10%), the chlorine mass fraction in the biomass (0.35%, 1%, 2%) and the Ca:S mole ratio (2.5, 4) are reported and discussed in the paper, for two specific fuels: high sulfur lignite and high chlorine corn stover. Concerning SO_2 emissions a correlation among the sulfur and the chlorine contents is clearly detected, being affected by the direct desulfurization mechanism occurring under oxy-firing conditions. The single effect of the chlorine content is found to be almost 1.5% of the desulfurization efficiency. NO_x emissions are otherwise more dependent on oxygen excess and CO concentration in the reactor, rather than the fuel share or the chlorine supplied. Thick deposition is only detected when chlorine content in the corn is 2%. Potassium

[1] Corresponding author, e-mail address: luisig@unizar.es

aluminosilication is found to be enhanced in comparison to potassium sulfation under oxy-firing, especially for the highest Ca:S mole ratio: observed aluminosilication is five times higher when Ca:S ratio is increased from 2.5 to 4. A significant enrichment in iron is also detected for the fly ash composition, with an increase of 30-50% in comparison to air combustion.

Keywords

Emissions, Deposition, Ashes, Co-firing, Bio-CCS, Fluidized beds; Lignite; Zea mays stover

1. Introduction

During the last ten years, oxy-fuel combustion has been proven to be a driving technology towards zero emission power plants [1]. Successful experiences have been reported in pulverized-fuel facilities, as Schwarze Pumpe, Ciuden and Callide [2–6]. Application to fluidized bed boilers has also shown promising results in similar scales [7, 8], with the inherent advantages of wide fuel flexibility and low pollutant emissions. According to these developments, oxy-combustion units are ready to get a commercial scale [9].

More recently, biomass has been proposed to be used as main or secondary fuel in oxy-fired units, aiming to develop bio-CCS (Carbon Capture and Storage with biofuels) [10, 11]. While conventional combustion of biomass has been extensively studied [12–14], few oxy-combustion experiences are available to date [15]. The permanent disposal of CO_2 from the combustion of residual biomass contributes to remove CO_2 from the atmosphere, leading to the so-called negative emissions. This enhances the attractiveness of the oxy-combustion technologies.

In comparison to coal, firing biomass shows several challenges mainly related to its chemical composition, strongly affected by issues like harvesting, soil residues or use of fertilisers [16]. Main operational problems

are related to the presence of alkalis and chlorine, which promote deposition on heat transfer surfaces and can also yield long-term corrosion [17–20].

Co-firing of coal and biomass can be considered as an intermediate way to mitigate these problems [21], also enabling the feeding of biomass into larger units [22]. Nevertheless, the synergies between the mineral matters of the fuels have to be well determined. The presence of the sulfur in the coal promotes the reactions between sulfur oxides and alkali chlorides, yielding chlorine-free deposits; the reactions (R.1) and (R.2) show this effect:

$$2\,MCl + SO_2 + {}^1\!/_2\,O_2 + H_2O \rightarrow M_2SO_4 + 2\,HCl \qquad \text{R. 1}$$

$$2\,MCl + SO_3 + H_2O \rightarrow M_2SO_4 + 2\,HCl \qquad \text{R. 2}$$

Following this reduction mechanism, Kassman et al. [23, 24] reported the effect of injecting ammonium sulfate, resulting in a decrease of the chlorine detected in the deposits. SO_2 oxidation rate (to SO_3) was suggested by these authors as the limiting factor for the alkali sulfation, since reaction R.2 eventually controls the process.

On the other hand, alkalis can also be competitively retained in the coal ashes by silication or aluminosilication [21], releasing chlorine to the gas-phase as HCl, according to the reactions (R.3) and (R.4):

$$2\,MCl + nSiO_2 + H_2O \rightarrow M_2O \cdot n\,SiO_2 + 2\,HCl \qquad \text{R. 3}$$

$$2\,MCl + (nSiO_2 + Al_2O_3) + H_2O \rightarrow 2\,MAlSi_{n/2}O_{(n+2)} + 2\,HCl \qquad \text{R. 4}$$

According to the results given by Sevonius et al. [25], the extent of reaction R.3 is very small at fluidized bed conditions and most of alkali retention is due to aluminosilication.

Few results are available in literature concerning co-firing under O_2/CO_2 atmospheres, most devoted to pulverized-fuel burners. Fryda et al. [26] pioneered the research on ash deposition under oxy-fuel conditions, finding out an increase of deposition ratios in comparison to air conditions, but

barely affecting the ashes composition. Riaza et al. [27] studied the co-firing of coal and olive residues in an entrained flow reactor, under a variety of O_2/CO_2 atmospheres. They reported an improvement of ignition temperature when biomass was added, and an opposite trend for NO_x emissions: increasing for semi-anthracite but decreasing for bituminous coals. Similar results were reported by Ahn et al. [28]. According to the scheme given by reactions (R.1) and (R.2), Ekvall et al. [29, 30] and Jurado et al. [31] respectively found an increase of K_2SO_4 in deposits and a decrease of SO_2 under oxy-firing of coal and biomass.

As concerns the experiences in fluidized bed combustors, most have been focused on emissions. Tan et al. [32] oxy-fired coal and wood pellets, showing a NO decrease with the biomass-to-coal ratio, without a conclusive trend for the SO_2. Duan et al. [33] found that NO emissions were strongly dependent on O_2 excess and O_2 primary/secondary split, as also happens for coal air- and oxy-firing.

This paper aims at widening the knowledge about oxy-firing of coal and biomass in fluidized bed reactors, focusing the analysis on emissions but also on the behaviour of the solid-phase: deposition ratios and composition, and ashes characterization. This is done for blends of two risky fuels, high-sulfur lignite and high-chlorine corn stover, leading to novel results not available up to now.

2. Experimental setup

2.1 *Facility*

The tests were conducted in the fluidized bed reactor at CIRCE Laboratories (Figure 1). The reactor is 2.5 m height and its inner diameter is 0.203 m. Fuel is fed from two independent hoppers, discharging into two variable-speed endless screws. Bed temperature is regulated by water-cooled probes, which can be inserted/extracted on-load. Further details of the facility can be found elsewhere [34–36].

The installation is instrumented with temperature, pressure and flow meters, providing real-time information about the unit performance. Flue gas composition (CO_2, CO, NO, SO_2, O_2) is also available, by sampling and analysing at the heat exchanger outlet.

An air-cooled deposition probe can be introduced over the splash zone, in order to characterize the deposits. Probe temperature is controlled to maintain a value within 450-500ºC. A removable coupon is inserted in the tip of the probe, in order to proceed with a subsequent SEM/EDX analysis. Solid samples can be taken during the experiments from the bed bottom, the baffle chamber and the cyclone.

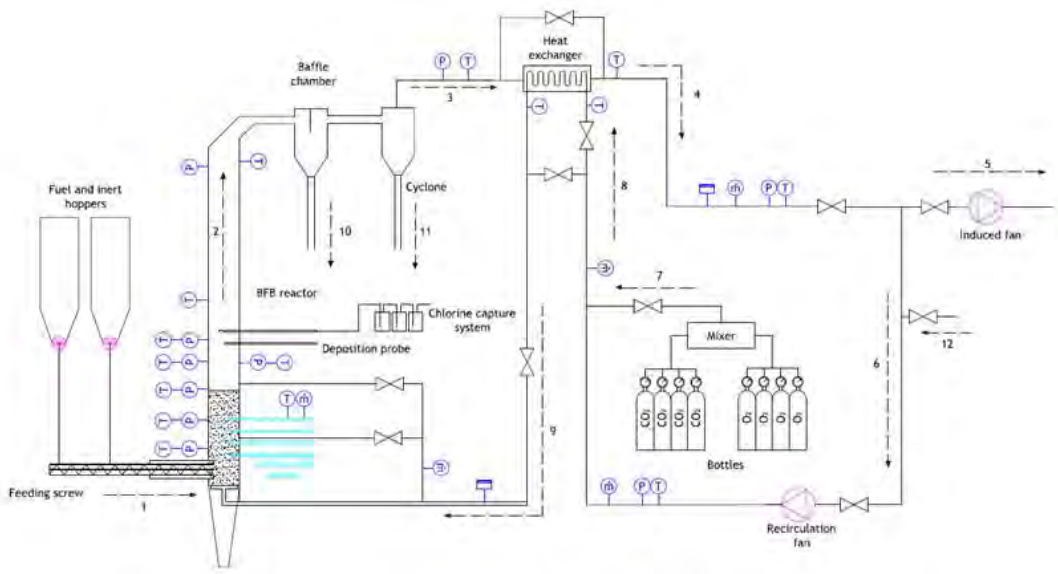

Figure 1.- Oxy-fired fluidized bed facility.

The presence of chlorine in the gas-phase can be determined by conveying samples through three Na_2CO_3 impingers. The sample withdrawal is carried out at 0.9 m over the distributor plate. After every experiment, the contents of the impingers are analysed by ion chromatography (IC) in order to determine the chloride concentration.

2.2 *Fuels*

The fuels selected for the experimental campaign were lignite and corn stover. The former is high-sulfur, high-ash coal with large reserves in Spain. The latter is an agricultural residue, selected to seek the interactions among chlorine and sulfur compounds.

	Lignite	Corn Stover
Mass fractions (%) as received		
Water	13.57	6.18
Ash	30.30	5.50
Chlorine	–	0.35
LHV as received (MJ kg^{-1})	14.43	15.44
Proximate analysis		
mass fractions (%) m.a.f.		
Volatiles	45.82	80.03
Fixed carbon	54.18	19.97
Ultimate analysis		
mass fractions (%) m.a.f.		
C	72.21	49.03
H	5.67	6.59
N	0.50	0.65
S	11.85	0.12
Ash oxide mass fractions (%)		
determined by ICP		
Al_2O3	26.01	1.36
CaO	3.27	8.72
Fe_2O3	22.23	6.08
K_2O	0.92	27.90
MgO	0.96	3.27
Na_2O	0.12	0.22
SiO_2	41.06	29.81
TiO_2	0.76	0.80
P_2O_5	–	3.81
MnO_2	–	0.14

Table 1.- Fuel analysis, heating value and ash composition.

The coal was supplied by a Spanish mining company. The coalfield is located close to Ariño (Teruel, Spain). The coal was sent to an Italian company in order to mill and sieve it to the required size. Round-trip transportation was done by truck. Once received back, chemical analysis was conducted to random samples of the coal, yielding proximate and ultimate analyses as well as heating values and ash composition (shown in Table 1). According to the classification given by the standard ASTM D388, the coal type is lignite. Its size was in the range 0.3–1 mm, with a mean diameter of 0.7 mm.

The corn stover was supplied by a local farmer from Villamayor (Zaragoza, Spain). Geo-coordinates of the field are 41º 41' 17" N, 0º 45' 45" W. Soil type is silty clay. The specific variety of Zea mays is unknown. Sowing was done during the early spring and harvesting during the early fall (year 2013). Corn stover bales were stored indoors by the farmer. We directly picked up and transported the bales from the field to the lab building. Since Zea mays cultivars cannot be completely specified, there is a reasonable concern that there may be factors that influence the results obtained, and for this reason the work cannot be independently reproduced. But the authors believe that the research exemplifies the effect of the inorganic constituents of both the coal and corn.

Corn stover was milled and sieved between 1 mm and 2 mm. Roughly, half of the initial mass was retained for the experiments. Chemical analysis was conducted to random samples of the sieved stover (results shown in Table 1). Fuels were separately stored in closed containers inside the lab building, at room temperature. The same was done with the limestone and the silica sand used in the tests.

The chlorine content in the corn stock (0.35%) was relatively low in comparison to the values reported in other works [37–39]. For this reason, original corn stover was doped with KCl, increasing the chlorine mass fraction to 1% and 2%. This consequently increased the content of mineral matter in the corn stover (to 6.80% and 8.80% respectively), while the rest of the proximate and ultimate fractions were reduced in proportion. To exclude

the effect of the moisture and the ash contents in the fuels, compositions in Table 1 are expressed in dry and ash-free basis.

In order to control SO_2 emissions, Granicarb limestone was added during the tests in different Ca:S mole ratios. This limestone is commercialized by a gravel plant located at Belchite (Zaragoza, Spain). Granicarb limestone is characterized by its high purity and reactivity ($CaCO_3$ > 97%). Limestone mean size was 0.6 mm. Silica sand (SiO_2 > 99 %) was used as inert material in the bed, with mean particle size similar to limestone. Bed height was maintained around 400 mm for all the tests.

2.3 *Experimental matrix*

Six experiments were conducted, according to the conditions given in Table 2. The matrix was defined to make possible the discussion of every independent influence. Air and oxy-fired (30/70% volume fractions O_2/CO_2) tests were completed, for a similar thermal input (about 22 kW). The fuels were blended in 80/20% and 90/10% coal-to-stover (LHV) ratios, firing three different corn stover samples. Two different Ca:S mole ratios were also tested, 2.5 and 4.

The facility is preheated by a propane burner up to T_{bed} ~ 500ºC, and then an air-combustion stage quickly raises the temperature to T_{bed} ~ 850ºC. Then, the firing is switched to O_2/CO_2 atmosphere. Once the operation is stable, deposition probe is inserted and chlorine-capture device is turned on. Operating data were gathered every two seconds during at least one hour and a half of steady-state conditions.

2.4 *Analytical techniques*

Hitachi S-3400N microscope equipped with a SDD-EDX detector Rontec XFlash was used to determine the composition and morphology of the particles taken from different sections of the facility (bed bottom, deposition probe, baffle chamber, cyclone). For that, a portion of each sample was disposed onto the holder carbon tape, micrographs were taken with the microscope and areas of interest were chosen for EDX analysis. For solid

202 mixtures as those found in the bed bottom, a number of particles were
203 selected (five from each type: sand, sorbent and ash), and composition of a
204 rectangular area of image was recorded. For finer powders as fly ash or
205 deposits, areas of interest were selected from SEM images to perform the
206 EDX analysis ensuring complete characterization.

207 The composition of the crystalline species was given by X-ray diffraction
208 (XRD) in a Siemens Bruker D8 Advance Series 2 diffractometer, set to select
209 Cu Kα radiation. The diffraction angle scanned was 20–70° 2 θ using a step
210 size of 0.05° 2 θ. Ion Chromatography (IC) was used to detect the presence of
211 soluble chlorides in the traps.

212

213

	A1	**OXY1**	**OXY2**	**OXY3**	**OXY4**	**OXY5**
Fluidizing gas, volume fractions	Air	30/70	30/70	30/70	30/70	30/70
Coal-to-biomass energy input ratio	80/20	80/20	80/20	90/10	80/20	80/20
Ca:S mole ratio	2.5	2.5	2.5	2.5	4	4
Chlorine mass fraction (%)	1	1	2	1	0.35	1
T_{bed} (ºC)	876	856	859	852	851	862
T_{fb} (ºC)	638	637	621	563	589	605
u_f (m s^{-1})	1.18	0.82	0.80	0.74	0.70	0.72
O_2 (%)	5.66	5.85	5.34	3.42	1.61	2.31
CO (mg m^{-3})	1139	746	863	473	417	908
NO (mg m^{-3})	240	343	348	514	504	289
NO (mg MJ^{-1})	46	37	40	59	54	33
SO_2 (mg m^{-3})	2207	12155	11078	13493	9790	8671
SO_2 (mg MJ^{-1})	455	1413	1382	1684	1111	1073
Desulfurization eff. (%)	87.7	61.7	62.9	59.5	70.2	71.4
Cl^- (mg m^{-3})	66.06	62.78	149.67	61.28	7.91	89.06

214 **Table 2.-** Operating conditions during the tests. CO, NO and SO_2 corrected to
215 6%O_2 and Normal conditions (273 K and 101.3 kPa)

216

217

3. Results and discussion

3.1 *Gas-phase*

Table 2 shows the mean values of the flue gas composition (O_2, CO, NO, SO_2), the operating temperatures and the fluidization velocities during every test, and as well as chlorine concentrations in the gas-phase and desulfurization efficiencies. Bed temperature was maintained within 850–880ºC, while O_2 concentration in flue gases mostly depended on the air/gas flowrate supplied to the reactor, which is proportional to the fluidization velocity. Under oxy-firing conditions, fluidization velocities were in the range 0.70–0.82 m s^{-1}. Velocity was higher under air-firing conditions (1.18 m/s), since the lower O_2 concentration (21% vs. 30%) requires an increase the air flowrate supplied for the same fuel load.

3.1.1 *SO_2 and NO emissions*

Taking into account the fuel rate supplied and the SO_2 concentration in flue gases, desulfurization efficiency was calculated after the tests. A value of 87.7% was obtained for the air-fired test, which is in good agreement with previous experience [35, 40]. It is clearly seen in the Table 2 that desulfurization efficiency drops during oxy-fired tests (16-28% efficiency points). This can be explained by the different sulfation processes taking place in the reactor. Under air-firing conditions, desulfurization takes place by means of an indirect capture mechanism. Firstly, limestone is calcined and then, the resulting CaO is sulfated (R.5 and R.6):

$$CaCO_3 \leftrightarrow CaO + CO_2 \qquad \text{R. 5}$$

$$CaO + SO_2 + {}^1/_2\, O_2 \rightarrow CaSO_4 \qquad \text{R. 6}$$

However, the conditions tested during oxy-fired tests (70% CO_2, T_b ~ 850ºC) imply a shift of the desulfurization mechanism. Limestone is not calcined, taking place the so-called direct desulfurization:

$$CaCO_3 + SO_2 + {}^1/_2\, O_2 \rightarrow CaSO_4 + CO_2 \qquad \text{R. 7}$$

The direct mechanism has been reported to result in lower desulfurization efficiencies by other researchers [41, 42], which is consistent with the numbers shown in Table 2. Therefore, operation of oxy-fired fluidized bed would require an increase of the Ca:S ratio in comparison to the experiences available for air-fired units. This is confirmed by the values in Table 2: if OXY1 is compared to OXY5, an efficiency increase of almost 10% efficiency points is observed when increasing Ca:S ratio from 2.5 to 4 (the rest of conditions remaining the same).

SO_2 emissions are also affected by the chlorine content supplied with the biomass. The higher the chlorine, the lower the SO_2 emitted, as can be seen if test OXY1 (1%) is compared to OXY2 (2%), or OXY4 (0.35%) to OXY5 (1%). This can be a consequence of alkali sulfation (R.1 and R.2), as discussed hereinafter.

As concerns actual NO emissions (mg m^{-3}, in Normal conditions), the lowest value is detected during the air-fired tests, provided that the flue gas flowrate (m^3 s^{-1}) is higher [43, 44]. Furthermore, air operation results in the top value for CO emissions, which is known to contribute to NO depletion (by direct reduction or by catalysing the heterogeneous reaction char + NO) [45–47]:

$$NO + CO \rightarrow CO_2 + {}^1/_2 N_2 \qquad \text{R. 8}$$

$$C_{char} + NO \rightarrow CO + {}^1/_2 N_2 \qquad \text{R. 9}$$

The highest value of CO concentration observed for the air-fired test can be explained by the fluidization velocity, yielding a lower residence time of the particles in the dense zone. In general, a good correlation can be observed between CO concentration and fluidization velocity, except for the test OXY5. This is not due to either the chlorine content in the corn or the Ca:S mole ratio, but to some uncontrolled instabilities in the fuel supply during the last test.

To avoid the effect of the different flue gas flowrates, emissions are usually compared in normalized units (mg MJ^{-1}). The reason relies on the

different $\%O_2$ contents that can be supplied with the gas mixture O_2/CO_2 as explained before. On the contrary to air combustion (fixed 21% O_2), oxy-combustion can be conducted with enriched O_2 concentrations. The rising of the O_2 concentration means a decrease of the supplied O_2/CO_2 total flowrate —for the same stoichiometric ratio, i.e. oxygen excess— and consequently a decrease of the flue gases flowrate.

If comparison is therefore done in normalized units (mg MJ^{-1}), then oxy-fired test OXY1 results in lower NO emissions than air-fired test A1 despite the higher $\%O_2$ supplied (the rest of conditions remaining the same). This trend is commonly found in open literature and it is explained by the high CO_2 concentration in the dense phase, contributing to an increase of char gasification, release of CO and subsequent NO reduction [40, 48, 49]. Guedea et al. [50] estimated the effect of gasification as an increase of 5-15% of the initial solid conversion in comparison to air conditions, for typical particle sizes in fluidized beds. Czackiert et al. [51] reported that CO represented 20% of the carbon conversion in the dense zone, for similar operating conditions (O_2/CO_2 atmosphere, temperature).

On the other hand, it is well known that free CaO catalyses NO formation [52], but this effect was very limited during our oxy-fired tests. According to the experimental values ($\%CO_2$ and bed temperatures), the tests were conducted under non-calcining conditions and then the presence of CaO can be considered negligible in comparison to $CaCO_3/CaSO_4$. This is not the case of the air-fired test, in which calcining conditions occurred, being another cause of the higher NO emission in (normalized) comparison to the test OXY1.

No significant influence of corn chlorine content on NO emissions can be observed if test OXY1 is compared to test OXY2: doubling the chlorine supplied, the NO emissions remain almost the same (for similar CO values). The same can be said for the Ca:S ratio: test OXY5 shows a very small reduction of NO emissions in comparison to the test OXY1 (Ca:S = 4 vs. Ca:S = 2.5).

3.1.2 *Chlorine concentration*

As explained before, gas samples were conveyed through three impingers in order to detect the chlorine concentration in the gas-phase. This is a useful indicator of the combined extent of sulfation and aluminosilication processes taking place in the reactor, since it is proportional to the HCl concentration in the gas-phase —also KCl aerosols and Cl_2 can be present in the trapped samples—. Chlorine concentration in the gas-phase (see Table 2) can be qualitatively correlated to the analysis carried out to the solid samples (ashes and deposits).

Chlorine was trapped in all tests, showing almost the same value if only the atmosphere is changed (air vs. O_2/CO_2). Under oxy-firing, the observed trend is the expected according to the chlorine content in the corn stover: test OXY2 shows the highest value, test OXY4 shows the lowest value. The reduction of the biomass in the fuel blend (10% OXY3 vs. 20% OXY1, both with 1% Cl) barely diminishes the chlorine detected in the gas-phase. A significant influence is nevertheless observed if OXY1 and OXY5 are compared, when only Ca:S ratio was modified. Cl^- concentration raises almost 50%, related to an increase of aluminosilication ratios as discussed in the next section.

3.2. Solid-phase

3.2.1. Bottom bed

Bottom bed solids collected after the tests are comprised by a mixture of particles rich in calcium (sorbent), particles rich in silica (sand) and particles rich in aluminosilicates (ashes). Surface composition of the three types of solid particles was studied by SEM-EDX, and elemental composition normalized to main elements is shown in Figure 2.

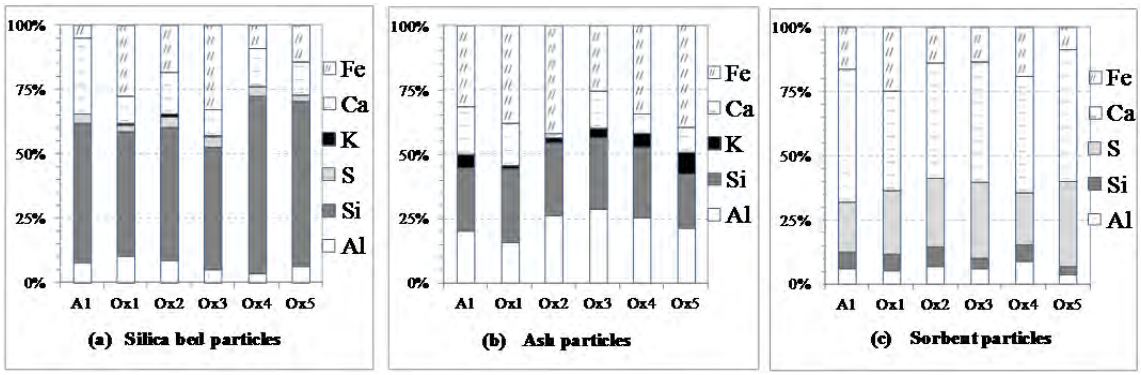

329

330 **Figure 2.-** Normalized composition of bottom bed solids (% mass fraction) by EDX.

331 An example of silica sand particles is shown in Figure 3.a, where it is
332 possible to see that they are covered by fine ash from extraneous and
333 inherent fuel mineral matter (Al, Fe), and fine matter from sorbent (S and
334 Ca). Small presence of potassium can be detected in some of the tests.

335 Coal ash particles are composed by Al-Si material and Ca and Fe fines,
336 Figure 3.b. No chlorine was detected in the bottom bed ashes during the
337 whole campaign. This was expectable, due to the high volatility of KCl.
338 Some sulfur was self-retained by the ashes, linked to Ca and Fe.

339 Particles rich in calcium and sulfur are considered partially sulfated
340 sorbent, see Figure 3.c. Surface composition in Figure 2 is not an accurate
341 indication of sulfation degree since only the external layer is analysed;
342 nevertheless, the information obtained by means of EDX indicates that fine
343 dust is covering the particles composed of aluminosilicate ash from
344 extraneous fuel mineral matter, and iron from inherent lignite mineral
345 matter as pyrite.

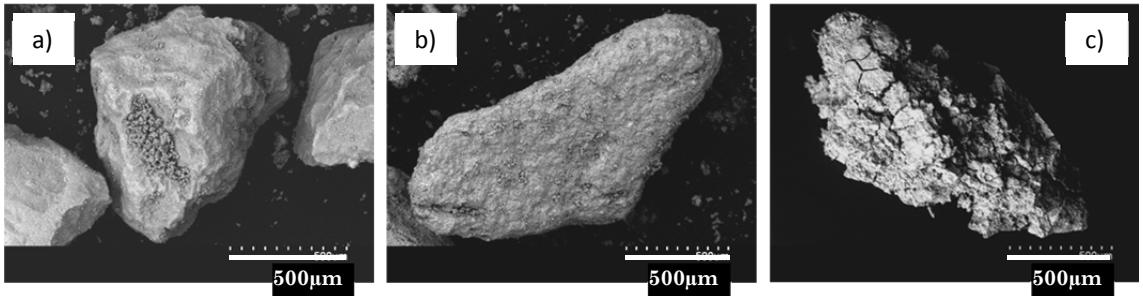

346

347 **Figure 3.-** Bed particles from test A1: (a) silica sand, (b) coal ash, (c) partially
348 sulfated sorbent.

349 The most important finding from EDX ash composition is the extent of
350 potassium presence on ash surfaces. To further study the interactions
351 between potassium and bed materials, some XRD analysis were performed
352 to bed solids collected during tests A1 and OXY1. The diffractograms are
353 shown in Figure 4.a. The most intense peak for both samples is quartz,
354 while the presence of sulphated sorbent as $CaSO_4$ is clear. On the other
355 hand, CaO is present in A1 solids whereas uncalcined $CaCO_3$ is present for
356 test OXY1 (as expected, due to the different desulfurization mechanism).
357 The diagrams do not identify any specie based on Fe, Al–Si nor species
358 where K would be chemically bound to aluminosilicates or silica. In fact,
359 calcination of lignite ashes in lab-scale furnace indicates that the original
360 crystalline aluminosilicate mineral matter develops into an amorphous
361 phase, since it is not detected in 850ºC ashes (Figure 4.b). In consequence,
362 EDX composition of surfaces is considered more representative than XRD to
363 the purpose of analysing interactions of different elements in coal and
364 biomass mineral matters.

365 Table 3 shows K/Si and K/Al mole ratios, in order to analyse the
366 interactions among the mineral matter. The ratios K/Si and K/Al of test A1
367 show a clear increase from those values in original coal ash, which points
368 out the incorporation of potassium in amorphous aluminosilicates. Test
369 OXY1 and OXY2 show a slight increase, whereas the increase is
370 outstanding for the cases OXY4 and OXY5 (Ca:S = 4). These results indicate
371 that for those test with high desulfurization efficiency, the reduction of SO_2
372 yields a decrease of alkali sulfation that may involve an increase of
373 potassium aluminosilication in the dense zone, according to reaction R.4.

374

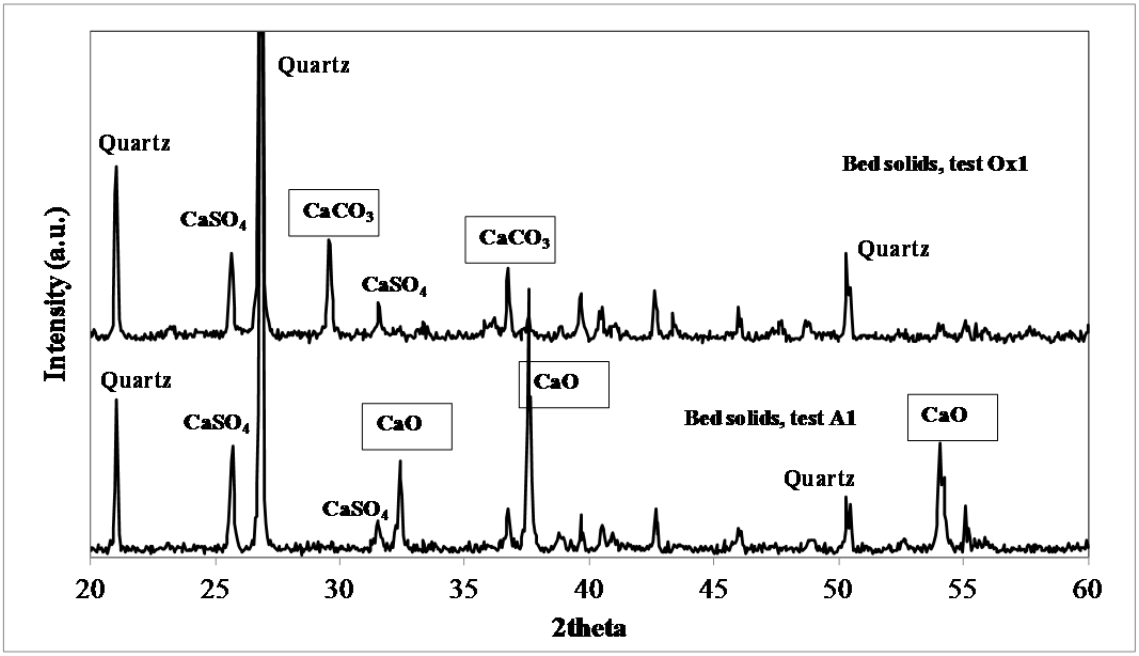

375

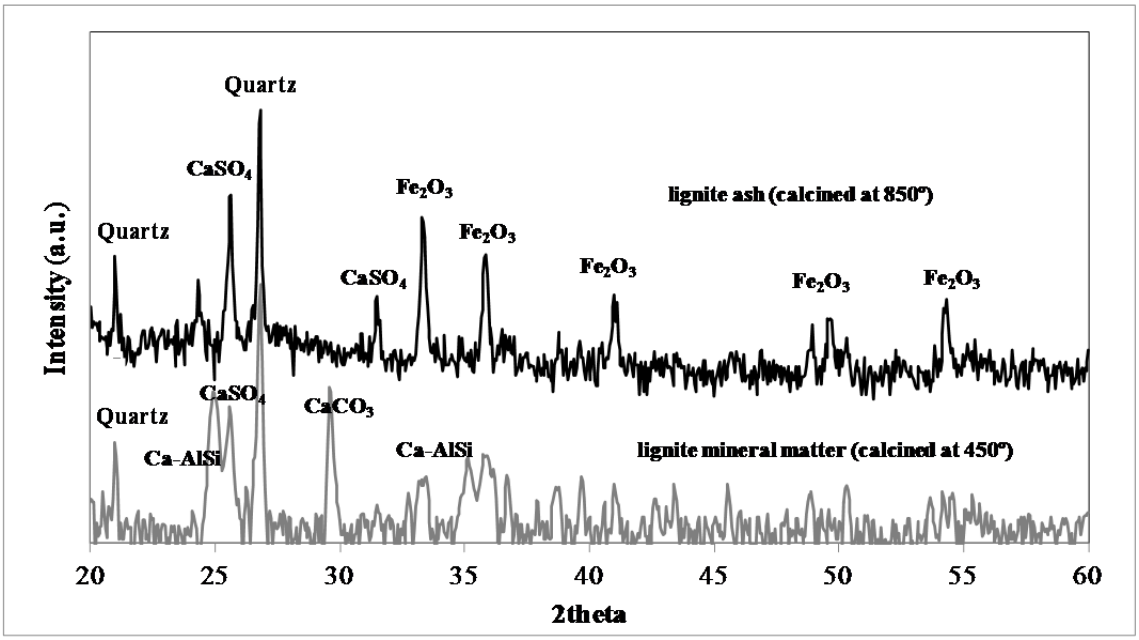

376

377 Figure 4.- XRD analysis of: (a) bed solids from tests A1 and OXY1, (b) mineral
378 residue after lignite ashing at 450º and 850ºC.

379

380

381

Test #	Particles	K/Si	K/Al
–	Original coal ash	0.027	0.038
A1	Bed ashes	0.149	0.175
OXY1	Bed ashes	0.031	0.056
OXY2	Bed ashes	0.049	0.051
OXY3	Bed ashes	0.093	0.087
OXY4	Bed ashes	0.131	0.136
OXY5	Bed ashes	0.293	0.272

Table 3.- Mole ratios in ashes collected from the bed bottom.

On the other hand, the decrease of biomass in the fuel share in test OXY3 also resulted in an enhancement of potassium aluminosilication, despite the larger SO_2 concentration from the coal. This could seem a contradiction, but there is another variable also playing a role: O_2 concentration. Several researchers [24, 53] have discussed that alkali sulfation is limited by an intermediate reaction, the oxidation of SO_2 to SO_3. This is a slow reaction at typical fluidized bed temperatures and highly dependent on O_2 concentration [54]. Therefore, if O_2 concentration diminishes, retention of potassium by aluminosilicates is enhanced in comparison to retention by sulfate.

No agglomeration issues were found during the entire experimental campaign. Formation of agglomerates has been described in literature [55, 56] due to interactions with silica sand, but mostly when full-load is given by firing biomass (or residues). Combination of SiO_2 from bed material and low melting point of biomass ash can promote agglomeration of the solids. But this effect has not been observed in our experiments, due to the low feed ratio of biomass (20% on energy basis) and the high ash content of the lignite (over 30%). The solids inventory in the bed is then involving a different chemistry. First, there is less apportioning of biomass ashes to the bed and, secondly, reactivity is modified by the significant presence of aluminosilicates from the coal ashes.

3.2.2 *Fly ash*

EDX composition of a representative sample of fine solids gathered from the cyclone is shown in Table 4 for tests A1, OXY1, OXY2 and OXY5 (on-load extraction was not possible during tests OXY3 and OXY4 due to operational constrain). They are a mixture of Al-Si fly ashes, $CaSO_4$ sorbent particles elutriated form the reactor, and an important presence of iron.

Test#	Mg	Al	Si	S	K	Ca	Fe
A1	1.50	17.08	21.58	5.50	4.53	21.77	27.43
OXY1	1.90	14.84	20.18	6.04	3.22	18.07	35.76
OXY2	1.65	14.17	18.82	5.24	3.99	15.64	40.49
OXY5	0.46	23.15	25.07	1.28	2.57	8.26	39.21

Table 4.- Elemental mass fractions (%) by EDX.

SEM images of fly ashes from OXY1 and OXY5 tests are shown in Figure 5.a. and 5.b. It is possible to see the mixture of different types of solids, where the presence of 20 to 30 μm spheres is clearly seen. EDX composition of the spheres determined their composition as iron oxide; their spherical shape indicates that the iron particles from inherent pyrite originally had a molten state, which corresponds to FeO–FeS eutectic identified in oxy-combustion of coal [57]. Similar iron morphology is found in OXY1 bottom bed ashes, as shown in Figure 5.c.

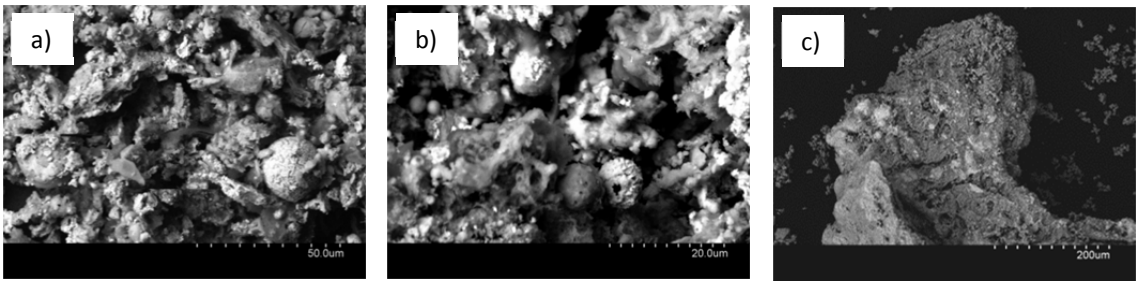

Figure 5.- SEM images of: (a) test OXY1 fly ash, (b) test OXY5 fly ash, (c) test OXY1 bottom bed ash.

Table 5 shows the calculation of K/Si and K/Al indexes according to the ash composition. For test A1 fly ash, the indexes show similar values than those found in bed particles. For the fly ash in oxy-combustion experiments, the trend is opposite to the bottom bed solids, since lower aluminosilication ratios are detected for the test OXY5 in comparison to OXY1. This is meaningful, since the potassium retained in the bed zone is not available beyond the splash zone. The amount of potassium found in fly ash in tests OXY1 and OXY2 can be related to the presence of condensed K_2SO_4 onto the elutriated particles.

Test #	Particles	K/Si	K/Al
–	Original coal ash	0.027	0.038
A1	Fly ash	0.151	0.183
OXY1	Fly ash	0.114	0.149
OXY2	Fly ash	0.152	0.194
OXY5	Fly ash	0.074	0.076

Table 5.- Element ratios in fly ashes collected from the cyclone.

3.3. Deposits

Some fuel-related indexes, based on empirical experiences, are widely used to predict the risk of deposition of alkali chlorides onto the heat transfer surfaces in combustion systems. The first index relates the sulfur and chlorine contents, S/Cl. Values over 4 are considered adequate, since alkalis can be sulfated and then chlorine is released to the gas-phase as HCl [21]. In the case of a fluidized bed reactor, this index has to be calculated taking into account that sorbent is usually added, and then sulfur availability is reduced. In our case, a modified S*/Cl index has been calculated, taking into account the desulfurization efficiencies reported in Table 2. The second index relates the silicon and aluminium contents to the

sodium and potassium contents, (Si + Al) / (Na + K). Values over 10 are considered promoting potassium aluminosilication, thus avoiding the alkali chloride deposition [58, 59]. Table 6 summarizes the values of these indexes for the combination of fuels and compositions used during the tests, as well as the deposition rate observed in the probe inserted in the reactor. According to the numbers in Table 6, no chlorine should be expected in the deposits, even for the test OXY2 with the highest chlorine content.

Test#	S/Cl	S*/Cl	(Al + Si) /(Na + K)	Deposit on probe
A1	31.57	10.78	19.39	No deposits
OXY1	31.57	12.10	19.39	Thin fouling
OXY2	15.78	5.85	14.64	Fouling
OXY3	74.71	30.25	30.07	Thin fouling
OXY4	90.21	26.92	24.79	Thin fouling
OXY5	31.57	9.01	19.39	Thin fouling

Table 6.- Fuel-related indexes and deposition rates observed.

No deposit was found on the coupon in test A1. Deposits on the probe after the tests OXY1, OXY2 and OXY4 were analysed by SEM-EDX as representative of the three different initial corn compositions (Table 7). The surface analysis confirmed the absence of chlorine. Provided that Fe from coupon surface could overlap Fe content in deposits, elemental composition values were normalized to Al, Si, S, K and Ca.

Test#	Al	Si	S	K	Ca
OXY1	9.05	12.59	35.10	33.11	10.15
OXY2	4.39	3.96	33.03	50.51	8.11
OXY4	21.37	28.39	14.37	19.35	16.51

Table 7.- EDX normalized composition (% mass fraction) of deposits from tests OXY1, OXY2 and OXY4.

Deposits in test OXY1 are comprised by a mixture of K_2SO_4 and $CaSO_4$ along with some aluminosilicate fines. Morphology of deposit is shown in Figure 6.a, where it is also possible to identify small spheres of iron. For test OXY2 (2% chlorine in the corn, the most fouled case), the presence of K_2SO_4 is clearly detected. Crystals of potassium sulfate can be easily seen in Figure 6.b. No molten deposits were detected. For test OXY4 (0.35% chlorine in the corn), potassium sulfate is less relevant and aluminosilicates are the major constituent. These results are fully consistent with the chlorine contents in the fuel and the Ca:S ratios supplied during the experiments.

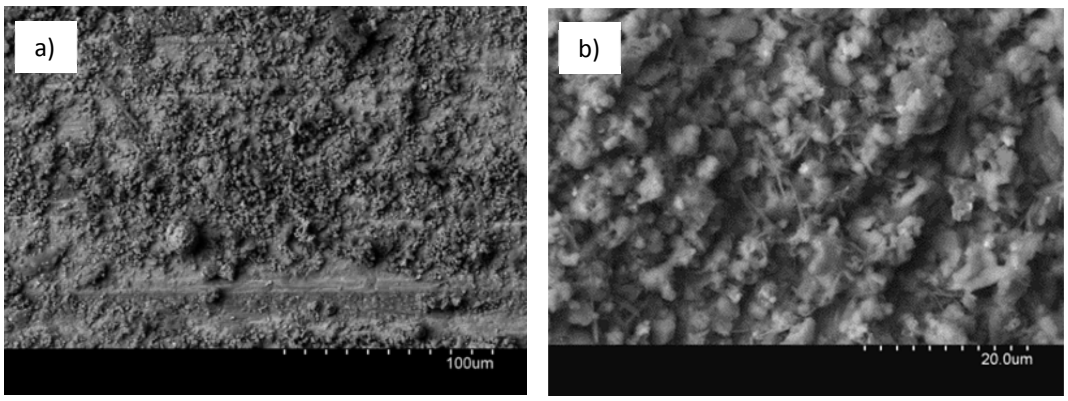

Figure 6.- SEM images of deposits: a) test OXY1, b) test OXY2.

4. Conclusions

SO_2 capture efficiency is affected not only by the O_2/CO_2 atmosphere, but also by the chlorine content supplied with the biomass. As concerns NO emissions, no relevant biomass-related influences are detected for the conditions tested.

Significant potassium contents in the bottom bed ashes have been found linked to amorphous aluminosilicates, especially for the oxy-fired tests with higher desulfurization efficiencies. As concerns fly ash composition, the presence of potassium is related to condensation of alkali sulfates on the solid surfaces. Oxy-firing largely increases the iron found in ash.

In relation to the deposits on the probe, no chlorine was detected even for the test with the largest deposition rates. The presence of K_2SO_4 in deposits has shown a consistent relation to the KCl content supplied with the fuel.

The observed results can be representative for large-scale fluidized bed boilers. Despite the differences in fluid dynamics, most of the phenomena addressed in our lab-scale research are related to the chemical conversions in the dense zone, and then comparative trends are meaningful.

Acknowledgements

The work described in this paper was partially funded by the R+D Spanish National Program from the Spanish Ministry of Economy and Competitiveness, under the Project ENE2012-39114. The project is also co-funded by the European Commission (European Regional Development Funds).

References

[1] R. Stanger, T. Wall, R. Spörl, M. Paneru, S. Grathwohl, M. Weidmann, et al., Oxyfuel combustion for CO_2 capture in power plants, Int. J. Greenh. Gas Control. 40 (2015) 55-125.

[2] T. Wall, R. Stanger, S. Santos, Demonstrations of coal-fired oxy-fuel technology for carbon capture and storage and issues with commercial deployment, Int. J. Greenh. Gas Control. 5 (2011) S5–S15.

[3] T. Yamada, T. Kiga, C. Spero, COP -Operational Resultsof Callide-A Oxyfuel Power Plant, in: 5th Meeting IEAGHG Int. Oxyfuel Combust. Res. Netw., Wuhan (China), 2015.

[4] R. Faber, J. Yan, F. Stark, S. Priesnitz, Flue gas desulphurization for hot recycle Oxyfuel combustion: Experiences from the 30 MW_{th} Oxyfuel pilot plant in Schwarze Pumpe, Int. J. Greenh. Gas Control. 5 (2011) S210–S223.

[5] M. Anheden, U. Burchhardt, H. Ecke, R. Faber, O. Jidinger, R. Giering, et al., Overview of operational experience and results from test activities in Vattenfall's 30 MW_{th} oxyfuel pilot plant in Schwarze Pumpe, Energy Procedia. 4 (2011).

[6] M. Lupion, B. Navarrete, P. Otero, V.J. Cortés, Experimental programme in CIUDEN's CO_2 capture technology development plant for power generation,

528 Chem. Eng. Res. Des. 89 (2011) 1494–1500.

529 [7] M. Lupion, R. Diego, L. Loubeau, B. Navarrete, CIUDEN CCS Project:
530 Status of the CO_2 capture technology development plant in power
531 generation, Energy Procedia. 4 (2011) 5639–5646.

532 [8] M. Gómez, A. Fernández, I. Llavona, R. Kuivalainen, Experiences in sulphur
533 capture in a 30 MW_{th} Circulating Fluidized Bed boiler under oxy-combustion
534 conditions, Appl. Therm. Eng. 65 (2014) 617–622.

535 [9] S. Santos, Future of Oxyfuel Combustion, in: 5th Oxyfuel Combust. Res.
536 Netw., Wuhan (China), 2015.

537 [10] P. Gładysz, A. Ziębik, Environmental analysis of bio-CCS in an integrated
538 oxy-fuel combustion power plant with CO_2 transport and storage, Biomass
539 and Bioenergy. 85 (2016) 109–118.

540 [11] S. Pickard, S.S. Daood, W. Nimmo, R. Lord, M. Pourkashanian, Bio-CCS: Co-
541 firing of Established Greenfield and Novel, Brownfield Biomass Resources
542 under Air, Oxygen-enriched Air and Oxy-fuel Conditions, Energy Procedia.
543 37 (2013) 6062–6069.

544 [12] S.G. Sahu, N. Chakraborty, P. Sarkar, Coal–biomass co-combustion: An
545 overview, Renew. Sustain. Energy Rev. 39 (2014) 575–586.

546 [13] Y. Niu, H. Tan, S. Hui, Ash-related issues during biomass combustion:
547 Alkali-induced slagging, silicate melt-induced slagging (ash fusion),
548 agglomeration, corrosion, ash utilization, and related countermeasures, Prog.
549 Energy Combust. Sci. (2015).

550 [14] M.E. Goerndt, F.X. Aguilar, K. Skog, Drivers of biomass co-firing in U.S.
551 coal-fired power plants, Biomass and Bioenergy. 58 (2013) 158–167.

552 [15] J. Riaza, R. Khatami, Y.A. Levendis, L. Álvarez, M. V. Gil, C. Pevida, et al.,
553 Combustion of single biomass particles in air and in oxy-fuel conditions,
554 Biomass and Bioenergy. 64 (2014) 162–174.

555 [16] M. Aho, A. Gil, R. Taipale, P. Vainikka, H. Vesala, A pilot-scale fireside
556 deposit study of co-firing Cynara with two coals in a fluidised bed, Fuel. 87
557 (2008) 58–69.

558 [17] P. Teixeira, H. Lopes, I. Gulyurtlu, N. Lapa, P. Abelha, Evaluation of
559 slagging and fouling tendency during biomass co-firing with coal in a
560 fluidized bed, Biomass and Bioenergy. 39 (2012) 192–203.

561 [18] J. Fagerström, E. Steinvall, D. Boström, C. Boman. Alkali transformation
562 during single pellet combustion of soft wood and wheat straw. Fuel Process.
563 Technol. 143 (2016) 204–212.

564 [19] H. Hagman, R. Backman, D. Boström. Effects on a 50 MW_{th} Circulating
565 Fluidized-Bed Boiler Co-firing Animal Waste, Sludge, Residue Wood, Peat,
566 and Forest Fuels. Energy & Fuels. 27 (2013) 6146–6158.

567 [20] D. Boström, N. Skoglund, A. Grimm, C. Boman, M. Ohman, M. Brostrom, R.

568 Backman. Ash transformation chemistry during combustion of biomass.
569 Energy & Fuels. 26 (2012) 85–93.

570 [21] M. Aho, E. Ferrer, Importance of coal ash composition in protecting the
571 boiler against chlorine deposition during combustion of chlorine-rich
572 biomass, Fuel. 84 (2005) 201–212.

573 [22] F. Al-Mansour, J. Zuwala, An evaluation of biomass co-firing in Europe,
574 Biomass and Bioenergy. 34 (2010) 620–629.

575 [23] H. Kassman, L. Bäfver, L.-E. Åmand, The importance of SO_2 and SO_3 for
576 sulphation of gaseous KCl – An experimental investigation in a biomass fired
577 CFB boiler, Combust. Flame. 157 (2010) 1649–1657.

578 [24] H. Kassman, J. Pettersson, B.M. Steenari, L.E. Åmand, Two strategies to
579 reduce gaseous KCl and chlorine in deposits during biomass combustion -
580 Injection of ammonium sulphate and co-combustion with peat, Fuel Process.
581 Technol. 105 (2013) 170–180.

582 [25] C. Sevonius, P. Yrjas, M. Hupa. Defluidization of a quartz bed – Laboratory
583 experiments with potassium salts. Fuel. 127 (2014) 161–168.

584 [26] L. Fryda, C. Sobrino, M. Cieplik, W.L. van de Kamp, Study on ash deposition
585 under oxyfuel combustion of coal/biomass blends, Fuel. 89 (2010) 1889–1902.

586 [27] J. Riaza, M.V. Gil, L. Álvarez, C. Pevida, J.J. Pis, F. Rubiera, Oxy-fuel
587 combustion of coal and biomass blends, Energy. 41 (2012) 429–435.

588 [28] S. Ahn, G. Choi, D. Kim, The effect of wood biomass blending with pulverized
589 coal on combustion characteristics under oxy-fuel condition, Biomass and
590 Bioenergy. 71 (2014) 144–154.

591 [29] T. Ekvall, F. Normann, K. Andersson, F. Johnsson, Modeling the Alkali
592 Sulfation Chemistry of Biomass and Coal Co-firing in Oxy-fuel Atmospheres,
593 Energy & Fuels. 28 (2014) 3486–3494.

594 [30] T. Ekvall, Alkali sulphation in flames, in: 5th Meeting IEAGHG Int. Oxyfuel
595 Combustion Res. Netw., Wuhan (China), 2015.

596 [31] N. Jurado, H.G. Darabkhani, E.J. Anthony, J.E. Oakey, Oxy-combustion
597 Studies Into the Co-Firing of Coal and Biomass Blends: Effects on Heat
598 Transfer, Gas and Ash Compositions, Energy Procedia. 63 (2014) 440–452.

599 [32] Y. Tan, L. Jia, Y. Wu, Some Combustion Characteristics of Biomass and Coal
600 Cofiring under Oxy-Fuel Conditions in a Pilot-Scale Circulating Fluidized
601 Combustor, Energy & Fuels. 27 (2013) 7000–7007.

602 [33] L. Duan, Y. Duan, C. Zhao, E.J. Anthony, NO emission during co-firing coal
603 and biomass in an oxy-fuel circulating fluidized bed combustor, Fuel. 150
604 (2015) 8–13.

605 [34] L.M. Romeo, L.I. Díez, I. Guedea, I. Bolea, C. Lupiáñez, A. González, et al.,
606 Design and operation assessment of an oxyfuel fluidized bed combustor, Exp.
607 Therm. Fluid Sci. 35 (2011) 477–484.

608 [35] C. Lupiáñez, L.I. Díez, L.M. Romeo, Influence of gas-staging on pollutant
609 emissions from fluidized bed oxy-firing, Chem. Eng. J. 256 (2014) 380–389.

610 [36] L.I. Díez, C. Lupiáñez, I. Guedea, I. Bolea, L.M. Romeo, Anthracite oxy-
611 combustion characteristics in a 90 kW_{th} fluidized bed reactor, Fuel Process.
612 Technol. 139 (2015) 196–203.

613 [37] D.A. Tillman, D. Duong, B. Miller, Chlorine in Solid Fuels Fired in
614 Pulverized Fuel Boilers — Sources, Forms, Reactions, and Consequences: a
615 Literature Review, Energy & Fuels. 23 (2009) 3379–3391.

616 [38] J.M. Johansen, M. Aho, K. Paakkinen, R. Taipale, H. Egsgaard, J.G.
617 Jakobsen, et al., Release of K, Cl, and S during combustion and co-
618 combustion with wood of high-chlorine biomass in bench and pilot scale fuel
619 beds, Proc. Combust. Inst. 34 (2013) 2363–2372.

620 [39] R. Hoskinson, D. Karlen, S. Birrell, C. Radtke, W. Wilhelm, Engineering,
621 nutrient removal, and feedstock conversion evaluations of four corn stover
622 harvest scenarios, Biomass and Bioenergy. 31 (2007) 126–136.

623 [40] C. Lupiáñez, I. Guedea, I. Bolea, L.I. Díez, L.M. Romeo, Experimental study
624 of SO_2 and NO_x emissions in fluidized bed oxy-fuel combustion, Fuel Process.
625 Technol. 106 (2013) 587–594.

626 [41] L.F. de Diego, A. Rufas, F. García-Labiano, M. de las Obras-Loscertales, A.
627 Abad, P. Gayán, et al., Optimum temperature for sulphur retention in
628 fluidised beds working under oxy-fuel combustion conditions, Fuel. 114
629 (2013) 106–113.

630 [42] L. Jia, Y. Tan, E.J. Anthony, Emissions of SO_2 and NO_x during Oxy−Fuel
631 CFB Combustion Tests in a Mini-Circulating Fluidized Bed Combustion
632 Reactor, Energy & Fuels. 24 (2010) 910–915.

633 [43] L.F. de Diego, M. de las Obras-Loscertales, A. Rufas, F. García-Labiano, P.
634 Gayán, A. Abad, et al., Pollutant emissions in a bubbling fluidized bed
635 combustor working in oxy-fuel operating conditions: Effect of flue gas
636 recirculation, Appl. Energy. 102 (2013) 860–867.

637 [44] C. Lupiáñez, L.I. Díez, L.M. Romeo, NO Emissions from Anthracite Oxy-
638 Firing in a Fluidized-Bed Combustor: Effect of the Temperature, Limestone,
639 and O_2, Energy & Fuels. 27 (2013) 7619–7627.

640 [45] H. Hosoda, T. Hirama, NO_x and N_2O Emission in Bubbling Fluidized-Bed
641 Coal Combustion with Oxygen and Recycled Flue Gas: Macroscopic
642 Characteristics of Their Formation and Reduction, Energy & Fuels. 12
643 (1998) 102–108.

644 [46] F. Scala, R. Chirone, Fluidized bed combustion of single coal char particles at
645 high CO_2 concentration, Chem. Eng. J. 165 (2010) 902–906.

646 [47] L. Duan, C. Zhao, Q. Ren, Z. Wu, X. Chen, NOx precursors evolution during
647 coal heating process in CO_2 atmosphere, Fuel. 90 (2011) 1668–1673.

648 [48] L. Jia, Y. Tan, C. Wang, Experimental Study of Oxy-Fuel Combustion and

649 Sulfur Capture in a Mini-CFBC, Energy & Fuels. 21 (2007) 3160–3164.

650 [49] L. Duan, C. Zhao, W. Zhou, C. Qu, X. Chen, O_2/CO_2 coal combustion
651 characteristics in a 50 kW_{th} circulating fluidized bed, Int. J. Greenh. Gas
652 Control. 5 (2011) 770–776.

653 [50] I. Guedea, D. Pallarés, L.I. Díez, F. Johnsson. Conversion of large coal
654 particles under O_2/N_2 and O_2/CO_2 atmospheres – Experiments and
655 modelling. Fuel Process. Technol. 112 (2013) 118-128.

656 [51] T. Czackiert, W. Muskala, S. Jankowska, G. Krawczyk, P. Borecki, L.
657 Jesionowski, W. Nowak. Combustible matter conversion in an oxy-fuel
658 circulating fluidized-bed (CFB) environment. Energy & Fuels 26 (2012) 5437-
659 5445.

660 [52] J.E. Johnsson. Formation and reduction of nitrogen oxides in fluidized-bed
661 combustion. Fuel 73 (1994) 1398-1414.

662 [53] S. Jiménez, J. Ballester, Formation of alkali sulphate aerosols in biomass
663 combustion, Fuel. 86 (2007) 486–493.

664 [54] L. Duan, Y. Duan, Y. Sarbassov, Y. Li, E.J. Anthony, SO_3 formation under
665 oxy-CFB combustion conditions, Int. J. Greenh. Gas Control. 43 (2015) 172–
666 178.

667 [55] Grimm, M. Öhman, T. Lindberg, A. Fredriksson, D. Brown. Bed
668 agglomeration characteristics in fluidized-bed combustion of biomass fuels
669 using olivine as bed material. Energy & Fuels. 26 (2012) 4550–4559.

670 [56] M. Bartels, W. Lin, J. Nijenhuis, F. Kapteijn, J.R. Ommen, Agglomeration in
671 fluidized beds at high temperatures: Mechanisms, detection and prevention.
672 Progress in Energy and Combustion Science. 34 (2008) 633-666.

673 [57] M.C. Mayoral, J.M. Andrés, M.T. Izquierdo, B. Rubio, Pyrrhotite deposition
674 through thermal projection to simulate iron sulphide slagging in oxyfuel
675 combustion, Fuel. 101 (2012) 197–204.

676 [58] K. Salmenoja, K. Makela, Superheater corrosion in environments containing
677 potassium and chlorine., J. Inst. Energy. 69 (1996) 155.

678 [59] E. Furimsky, L. Zheng, Quantification of chlorine and alkali emissions from
679 fluid bed combustion of coal by equilibrium calculations, Fuel Process.
680 Technol. 81 (2003) 7–21.